is substantially smaller than is the causative increase in the airflow rate. The surface temperature of the water is raised as the air temperature rises. Over the span of plenum temperatures T_p from 80° to 200°F., T_1 varies from about 47° to 83°F., essentially independent of N_{R2}.

ACKNOWLEDGMENT

The authors gratefully acknowledge the assistance of Yung-cheng Yu in various aspects of the numerical computations.

NOTATION

D = mass diffusion coefficient
D_e = equivalent diameter, $2H$
f = velocity function, Equation (6)
H = channel height
h = heat transfer coefficient, Equation (24)
K = mass transfer coefficient, Equation (25)
k = thermal conductivity
$\dot{m}$ = mass flow/time area
N_{Nu} = Nusselt number, hD_e/k
N_{Pr} = Prandtl number, ν/α
N_{R_2} = injection Reynolds number, v_2H/ν
$N_{R\bar{u}}$ = axial Reynolds number, $\bar{u}H/\nu$
N_{Sc} = Schmidt number, ν/D
N_{Sh} = Sherwood number, $KH/\rho D$
p = pressure
T = temperature
u = axial velocity
$\bar{u}$ = mean velocity
v = transverse velocity
W = mass fraction
x = axial coordinate
y = transverse coordinate

Greek Letters

α = thermal diffusivity
β = injection ratio, $-(v_1/v_2)$
η = dimensionless coordinate, y/H
λ = latent heat
ν = kinematic viscosity
ρ = density
Φ_T = temperature variable, $(T - T_1)/(T_2 - T_1)$
Φ_W = mass fraction variable, $(W_i - W_{i1})/(W_{i2} - W_{i1})$
Ω_T = Prandtl number
Ω_W = Schmidt number

Subscripts

i, j = mixture components
p = plenum chamber
1 = wall with lesser $|v|$
2 = wall with greater $|v|$

LITERATURE CITED

1. Berman, A. S., *J. Appl. Phys.*, **24**, 1232 (1953).
2. Terrill, R. M., and G. M. Shrestha, *ZAMP*, **16**, 470 (1965).
3. Terrill, R. M., *Intern. J. Heat Mass Transfer*, **8**, 1491 (1965).
4. Gill, W. N., Eduardo del Casal, and D. W. Zeh, *AIChE J.*, **12**, 266 (1966).
5. Huesmann, K., and E. R. G. Eckert, "Untersuchungen über die laminare Strömung und dem Umschlag zur Turbulenz in Porösen Rohren mit gleichmässiger Einblasung durch die Rohrwand," Vol. 1, p. 1, *Wärme- und Stoffübertragung*, Germany (1968).
6. Rodi, W., *Heat Transfer Lab. Rept. No. 79*, Univ. Minn., Minneapolis (Feb., 1968).
7. Sherwood, T. K., and R. L. Pigford, "Absorption and Extraction," McGraw-Hill, New York (1952).

Manuscript received November 4, 1968; revision received January 10, 1969; paper accepted January 14, 1969.

Initiation of Thermal Convection in Finite Right Circular Cylinders

IVAN CATTON and D. K. EDWARDS

University of California, Los Angeles, California

Linear perturbation analyses are extended to determine the lowest Rayleigh number at which convection initiates in a vertical cylinder heated on the bottom and cooled on the top. The critical Rayleigh number for the first mode of convection in a right circular cylinder with a perfectly conducting wall is shown to be three times larger than that in such a cell with a perfectly adiabatic side wall. An adjusted wave number is shown to make the results of Pellew and Southwell applicable to the adiabatic wall in a manner similar to that used by Pnueli and Ostrach for the perfectly conducting side wall. The results are compared with experiment and are in very good agreement.

It has long been known that a thermally expansive fluid enclosed between horizontal plates and heated from below starts to convect only when a critical temperature gradient is surpassed. After Benard's (*1*) observations, Rayleigh (2) gave a theoretical explanation of such a phenomenon, neglecting effects of surface tension and shear stress on the horizontal boundaries. Pellew and Southwell (3) found an exact solution to the linearized perturbation equations, taking account of shear at the horizontal boundaries.

Malkus (*4*) pointed out that not only is there a first critical Rayleigh number (as the critical dimensionless

temperature gradient has become known) but also successively higher critical Rayleigh numbers at which linearized perturbation theory predicts discrete transitions in the thermal convection. Malkus and Veronis (5) went on to apply a power integral technique to predict convection rates using approximate values of the critical Rayleigh numbers and integrals involving the velocity and temperature perturbations. Catton (6) repeated the Malkus and Veronis calculations using more exact values and found excellent agreement between theory and measurements of heat flux.

When lateral walls are present so that the fluid heated from below is completely confined, and when these walls are sufficiently close together to constrict the fluid convection, the first and higher critical Rayleigh numbers are increased greatly. Ostrach and Pnueli (7) have used Pellew and Southwell's technique of separation of variables to predict the first critical Rayleigh number for perfectly conducting lateral walls. Yih (8) has treated the infinite cylinder with perfectly insulated lateral wall, and Ostroumov (9) has given approximate relations for the first critical Rayleigh number in an infinitely long cylinder with arbitrarily conducting side wall.

Experimental measurements of the effect of lateral walls have been reported by Soberman (10), Globe and Dropkin (11), Ostroumov (9), Slavnov (12), and Catton and Edwards (13). Ostrach and Pnueli (7) also report measurements. These experimental results show either the first critical Rayleigh number or an influence of lateral walls on heat transfer rates. They do not indicate values of Rayleigh number at the higher discrete transitions. Excellent reviews of the thermal instability literature have been presented by Chandrasekhar (14) and Ostrach (15).

The object of this work is to obtain the first critical Rayleigh number for fluids between horizontal surfaces and enclosed by lateral walls. In what follows, cells with both perfectly conducting and perfectly insulating walls are treated in two limits, small cell height to lateral wall separation (low L/d) and large but not infinite L/d. The low L/d solution is obtained by Fourier analysis of the problem in the horizontal direction and the high L/d by Fourier analysis in the vertical direction. The low and high L/d solutions are then matched by relating the horizontal wave number to the aspect ratio through the boundary conditions (the adjusted wave number). Solutions are found for diametrically antisymmetrical flows in vertical circular cylinders, and a simple approximation is introduced to give Rayleigh number explicitly as a function of mode number and wave number.

THEORY OF INITIATION

Phenomena of Interest

Attention is focused on a thermally expansive fluid contained in a vertical right circular cylinder of arbitrary cross section and height L located in a downward directed gravity field. The flat bottom of the cylinder is heated to temperature T_h, and the flat top end is cooled to temperature T_c. It is known that if the density of the fluid near the hot surface becomes sufficiently lower than that near the cold surface, a steady natural convection will initiate in the cylinder. From physical reasoning it is expected that the vertical walls, when their characteristic horizontal separation distance d is of order L or smaller, will inhibit initiation by causing additional viscous damping and, if the walls are thermally conducting, by tending to eliminate temperature differences in any horizontal plane. It is desired to predict analytically the temperature difference required to initiate convection for a fluid with given properties contained in cells with either adiabatic or perfectly conducting side walls.

Governing Equations

To appreciate the limitations of the solutions obtained previously by others and the extensions made in the present work, it is necessary to consider the governing differential equations and most particularly the way in which the boundary conditions enter into the problem.

It is assumed that velocity, pressure, and temperature of the fluid are disturbed only slightly from those existing under conditions of no convection. Further, Sherman and Ostrach (16) have given a general proof that the principle of exchange of stabilities holds for this problem. Thus, if the time dependency of the disturbances is e^{pt}, then $p = 0$ at the point of neutral stability. These assumptions permit linearized, time independent equations governing the perturbations to be derived from conservation of mass, momentum, and energy:

$$\nabla \mathbf{v}' = 0 \tag{1}$$

$$0 = \mathbf{k}\alpha g T' - \frac{1}{\rho_0}\nabla P' + \nu \nabla^2 \mathbf{v}' \tag{2}$$

$$-w'\beta = \kappa \nabla^2 T' \tag{3}$$

where

$$\mathbf{v}'(x, y, z)e^{pt} = \mathbf{v}(x, y, z, t) \tag{4}$$

$$P'(x, y, z)e^{pt} = P(x, y, z, t) - P_0 + g\rho_0\left(z - \frac{1}{2}\alpha\beta z^2\right) \tag{5}$$

$$T'(x, y, z)e^{pt} = T(x, y, z, t) + \beta z - T_0 \tag{6}$$

$$\rho = \rho_0[1 - \alpha(T - T_0)] \tag{7}$$

$$T_0 = \frac{T_c + T_h}{2} \tag{8}$$

$$\beta = \frac{T_h - T_c}{L} \tag{9}$$

The pressure disturbance may be expressed in terms of the temperature disturbance by operating on the momentum equation, Equation (2), with the divergence operator and by making use of continuity, Equation (1):

$$\nabla^2 P' = \rho_0 \alpha g \frac{\partial T'}{\partial z} \tag{10}$$

A relation between the z component of velocity and the temperature may be obtained by taking the curl of Equation (2) twice and by writing the z component

$$\nu \nabla^4 w' = -\alpha g \nabla_\perp^2 T' \tag{11}$$

where the operator $\nabla_\perp^2$ is defined as

$$\nabla_\perp^2 = \nabla^2 - \frac{\partial^2}{\partial z^2} \tag{12}$$

Equation (11) may be used to eliminate temperature from the energy equation, Equation (3):

$$\nabla^6 w' = \frac{\alpha g \beta}{\kappa \nu}\nabla_\perp^2 w' \tag{13}$$

Equations (1) to (3) or the horizontal components of Equation (2) with Equations (11), (12), and (13) constitute a set of five equations with five unknowns, the three velocity components, and P' and T'. This set of equations will be solved for two asymptotic cases. The

first is where the side walls are far away (small aspect ratio) and contribute little to flow retardation. The second is where the top and bottom contribute little (high aspect ratio) to flow retardation. The effect of neglecting shear on horizontal or vertical surfaces on the critical Rayleigh number will depend on the aspect ratio. Both of the above limiting cases will be solved, and the range of validity of each case will be delineated in the discussion.

Boundary Conditions

Physical boundary conditions which should be satisfied are as follows:

$$\text{On all surfaces: } \mathbf{v}' = 0 \tag{14}$$

$$\text{Top and bottom: } z = \pm L/2,\ T' = 0 \tag{15}$$

$$\text{Adiabatic sides: } \mathbf{n} \cdot \nabla T' = 0 \tag{16}$$

$$\text{Perfectly conducting sides: } T' = 0 \tag{17}$$

Solutions, including those extensions developed in this work, have been obtained for simplified boundary conditions only. For example, if the sides are imagined to support no horizontal shear, Equation (14) may be replaced by

$$\text{Top and bottom: } \mathbf{v}' = 0$$

$$\text{Circular cylindrical side: } \frac{\partial v'_\theta}{\partial \theta} = 0,\ w' = 0 \tag{14a}$$

$$\int_A w' dA = 0$$

If the top and bottom are of much less area than the vertical side walls, and they are imagined to support no horizontal shear, Equation (14) may be replaced by

$$\text{Top and bottom: } w' = \frac{\partial u'}{\partial z} = \frac{\partial v'}{\partial z} = 0$$

$$\text{Sides: } \mathbf{v}' = 0 \tag{14b}$$

Solution for Low Height-to-Width Ratio

So that the characteristic equations may be cubic or lower in degree, to permit analytical solution, the exact boundary conditions are not satisfied; rather Equation (14*a*) is used in place of Equation (14). In cells with low height-to-width ratio, horizontal shear and normal flow through the side walls are imagined to have only small effects. This case was solved by Pellew and Southwell (3) for $L/d = 0$, and their result was used by Ostrach and Pneuli (7) for arbitrary L/d when the side walls are perfectly conducting, Equation (17). Appendix A contains a brief summary of the Pellew and Southwell solution and the derivation of a simple but accurate closed form approximation for Rayleigh number.

Table 1. Characteristic Rayleigh Numbers for Infinite Horizontal Surfaces

Wave number	Rayleigh number	Wave number	Rayleigh number
2.000	2177.4121	20.000	173573.46
3.116	1707.8617	22.000	250437.51
4.000	1879.2560	24.000	350803.52
6.000	3417.9828	28.000	640088.68
8.000	7084.5093	32.000	1081363.6
10.000	14134.439	36.000	1720707.3
12.000	26271.745	40.000	2610343.3
14.000	45599.428	44.000	3808639.6
16.000	74609.511	48.000	5380107.7
18.000	11617.991	52.000	7395403.8

Table 2. Critical Rayleigh Numbers for Horizontal Plates of Infinite Extent

	Wave number	Rayleigh number
Exact solution (Table 1)	3.116	1707.8
Approximate solution Equations (22) and (23)	2.823	1714.9

The solution is facilitated by Equation (14*a*) because horizontal harmonicity can be assumed:

$$\nabla_\perp^2 w' = -a^2 w' \tag{18}$$

The parameter a is related to the cell geometry and two horizontal wave numbers through the solution to Equation (18) and imposition of side wall boundary conditions. This determination of a is the key to applying Pellew and Southwell's results to making engineering estimates for $L/d > 0$.

When Equation (18) holds, separation of variables takes the form

$$w' = f_{mn}(x, y) g_k(z) \tag{19}$$

where $f_{mn}(x, y)$ is a solution to Equation (18), and $g_k(z)$ is a solution to Equation (13):

$$(D^2 - a^2)^3 g_k = -N_{Ra} a^2 g_k \tag{20}$$

where $D = d/dz$, and N_{Ra} is the Rayleigh number for a unit length L:

$$N_{Ra} = \frac{\alpha g \beta L^4}{\kappa \nu} \tag{21}$$

When the solution to Equation (20) is made to satisfy the top and bottom boundary conditions, a set of eigenvalues results from the secular equation. A member of the set is designated with subscript k. In the same way, there is a set of a values, a member of which is a_{nm}. The value a is chosen from this set by satisfying the side wall conditions $w' = 0$ and the continuity requirement $\int_A w' dA = 0$ and by minimizing N_{Rakmn}. As shown in Appendix A, an approximate explicit relation giving Rayleigh number N_{Rak} may be derived from the exact implicit relation presented by Pellew and Southwell. This convenient equation is

$$N_{Rak} = \frac{(a^2 + b_k^2)^3}{a^2} \tag{22}$$

$$b_k = k\pi + 0.85 \tag{23}$$

In the case of small L/d considered by Pellew and Southwell, any value of a is acceptable, since the influence of the side walls is negligible. In this case, the critical Rayleigh number is the lowest. Differentiating Equation (22) with respect to a and equating it to zero, we get

$$a^2 = b_k^2/2 \tag{24}$$

and substituting into Equation (23) we get

$$N_{Rak} = \frac{27}{4} b_k^4 \tag{25}$$

The results of extending Pellew and Southwell's calculations are presented in Table 1, and a comparison of the exact and approximate solutions is in Table 2. It can be seen that the approximate solution yields results that are within 1% of the exact results. Unfortunately it is not possible to satisfy Equation (18) with boundary conditions $w' = 0$ on the side walls without also imposing

TABLE 3. CHARACTERISTIC RAYLEIGH NUMBERS FOR CYLINDERS

Perfectly conducting walls L/d	Rayleigh Numbers	Adiabatic walls L/d	Rayleigh numbers
0.25	804.71999	0.25	776.13067
0.50	1436.5006	0.50	1057.5137
1.00	6116.6706	1.00	2800.5745
2.00	63982.545	2.00	22739.056
4.00	916381.54	4.00	298420.28
8.00	14259025.1	8.00	4532897.8
16.00	22659834.0	16.00	71592294.0

$T' = 0$ on the side walls by virtue of Equation (11). Thus only the perfectly conducting side wall can be accommodated in the low L/d case, unless L/d is so low that Equation (24) holds. For this case $a = 7.66\ L/d$, where d is the diameter of the cylinder (7).

Solution for High Height-to-Width Ratios

In the case of high L/d, Equation (14b) is used in place of Equation (14), since horizontal shear on the ends of the cylinder is negligible compared with the viscous dissipation brought about by the side walls. With this simplification, vertical harmonicity may be assumed:

$$D^2w' = -b^2w' \tag{26}$$

Separation of variables again takes the form of Equation (19), with g the solution to Equation (26):

$$g_k = \cos(k\pi z/L) \quad k = 1, 3, 5, \ldots$$
$$g_k = \sin(k\pi z/L) \quad k = 2, 4, 6, \ldots \tag{27}$$
$$b_k = k\pi/L \tag{28}$$

For a circular cylinder and odd k, the f function in Equation (19) is as follows:

$$\begin{aligned} w &= W(r)\cos(k\pi z/L)\cos(n\theta) \\ u &= U(r)\sin(k\pi z/L)\cos(n\theta) \\ v &= V(r)\sin(k\pi z/L)\sin(n\theta) \\ P' &= (2\rho_0\nu/d)\Lambda(r)\cos(k\pi z/L)\cos(n\theta) \\ T' &= (\beta d^2/4\kappa)F(r)\cos(k\pi z/L)\cos(n\theta) \end{aligned} \tag{29}$$

where subscripts r denote lengths based on radius $d/2$:

$$N_{Ra}^* = \frac{\alpha g\beta d^4}{16\kappa\nu}, \quad b_r = k\pi/L_r, \quad L_r = \frac{2L}{d}, \quad \frac{d}{2} = 1 \tag{30}$$

In cylindrical coordinates, the governing partial differential equations become ordinary differential equations. They are Equations (10), (11), and (13), the sum of the horizontal components of Equation (2), and the difference of the horizontal components of Equation (2) as follows:

$$\left(D_r'D_r - \frac{n^2}{r^2} - b_r^2\right)\Lambda = -b_rN_{Ra}^*F \tag{31}$$

$$\left(D_r'D_r - \frac{n^2}{r^2} - b_r^2\right)W = -N_{Ra}^*\left(D_r'D_r - \frac{n^2}{r^2}\right)F \tag{32}$$

$$\left(D_r'D_r - \frac{n^2}{r^2} - b_r^2\right)^3 W = N_{Ra}^*\left(D_r'D_r - \frac{n^2}{r^2}\right)W \tag{33}$$

$$\left(D_r'D_r - \frac{(n+1)^2}{r^2} - b_r^2\right)(U+V) = \left(D_r - \frac{n}{r}\right)\Lambda \tag{34}$$

$$\left(D_r'D_r - \frac{(n-1)^2}{r^2} - b_r^2\right)(U-V) = \left(D_r + \frac{n}{r}\right)\Lambda \tag{35}$$

The operators are

$$D_r = \frac{d}{dr}, \quad D_r' = \frac{d}{dr} + \frac{1}{r} \tag{36}$$

Conversion from N_{Ra}^* to N_{Ra} follows from the definitions, Equations (21) and (30):

$$N_{Ra} = 16(L/d)^4 N_{Ra}^* \tag{37}$$

Yih (8) solved Equation (33) for the case of the adiabatic side wall and $b_r = 0$ ($L/d = \infty$). In Appendix B, the procedure used to solve the above set for the perfectly conducting side wall and adiabatic side wall with arbitrary b_r is described. The lowest value of Rayleigh number for a disturbance which satisfies continuity is found to be that for $n = 1$, $k = 1$ and for the lowest root of the secular equation. Table 3 gives the results for perfectly conducting and adiabatic walls. The results at low L/d approach the results of the free-free problem of Rayleigh (2), namely a Rayleigh number of 656. It is well known that the lower limit is 1,707 when the horizontal surfaces are rigid. The useful range of the high L/d solution can only be determined by comparison with experiment or by matching to the low L/d solution which has a minimum Rayleigh number of 1,707.

THE EQUIVALENT WAVE NUMBER CONCEPT

An approximate expression for the Rayleigh number at which convection will initiate can be obtained from Equation (22) provided an appropriate value of the wave number a can be estimated. It is proposed that an equivalent a be estimated from the two known exact solutions at high L/d and low L/d. At infinite L/d we have $N_{Ra1\infty}$ which must equal, according to Equation (22), $a^4{}_{1\infty}$. At very low L/d we have Equation (24). An estimate of an equivalent wave number can therefore be made as

$$a^2 \doteq (b_1{}^2/2) + (N_{Ra1\infty})^{1/2} \tag{38}$$

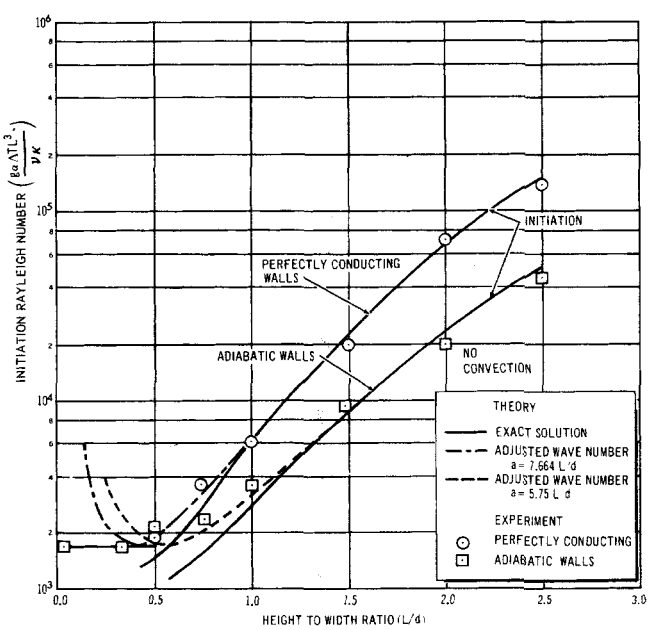

Fig. 1.

TABLE 4. CHARACTERISTIC RAYLEIGH NUMBERS FOR THE CYLINDER WITH FREE ENDS

	Perfectly conducting walls			Adiabatic walls		
L/d	Exact solution	Equation (41)	Discr.	Exact solution	Equation (41)	Discr.
0.5	1,436	1,306	−9%	1,057	929	−12%
1.0	6,116	6,237	+2%	2,800	2,828	+1%
2.0	63,982	64,817	+1%	22,739	23,051	+1%

TABLE 5. CHARACTERISTIC RAYLEIGH NUMBERS FOR THE INFINITE ROLL

L/H	This work	Yih	Samuels and Churchill*	Kurzweg*
0.5	1,714	750	1,840	2,016
1.0	2,490	1,600	2,460	2,540
2.0	12,860	11,280	11,600	12,120

* From Table 3 of reference 17.

where for rigid horizontal surfaces b_1 is given approximately by Equation (23) and for free (no shear) surfaces is simply π. The quantity N_{Ra1_∞} should be the value appropriate for the wall conductance. For the adiabatic wall, Yih's result of

$$N_{Ra1_\infty} = 16(67.9)\,(L/d)^4 \text{ adiabatic wall} \qquad (39)$$

should be used; for the perfectly conducting wall, the value of Ostrach and Pneuli

$$N_{Ra1_\infty} = (7.66\,L/d)^4 \qquad (40)$$

should be used; and for the arbitrarily conducting wall, a value from Ostroumov or Slavnov may be used.

Substituting the expression for the equivalent wave number, Equation (38), into Equation (22), we obtain

$$N_{Ra1} = \frac{2\left(\frac{3}{2}b_1^2 + N_{Ra1_\infty}{}^{1/2}\right)^3}{b_1^2 + 2N_{Ra1_\infty}{}^{1/2}} \qquad (41)$$

for the Rayleigh number at which convection will initiate.

To test this proposal we compare the values of N_{Ra1} given in Table 3 for finite L/d and free horizontal surfaces with values obtained from Equation (41) in Table 4. Agreement is seen to be within 10% in all cases.

DISCUSSION

The shortcoming which appears to raise the most serious questions about applying the results of the preceding analyses to real systems is the failure to satisfy all the boundary conditions. This failure does not appear to be too serious in the case of perfectly conducting walls, because the assumption of slippery and leaky side walls leads to a result in agreement with the exact solution as L/d approaches infinity, see Figure 1, and is inconsequential at $L/d = 0$ where the side walls have no influence.

The approximation, Equations (22) and (23), to Pellew and Southwell's exact result for $L/d = 0$ is seen to be good within approximately 1% in the critical Rayleigh number as shown in Table 2.

Patching the solution for high L/d onto the solution for low L/d through the equivalent wave number as in Equation (41) can hardly be defended from a theoretical point of view. However, Table 5 shows that as an estimation technique it yields results within 10% of the correct theoretical value for the cylinder with free ends and either conducting or adiabatic walls. It is interesting to note that the solution for the infinite roll between adiabatic walls obtained by Yih is $N_{Ra1_\infty} = (16)(31.29)(L/H)^4$, while for the infinite roll separation of variables via Equation (14a) gives $a = 2\pi\,L/H$, so that there results $N_{Ra1_\infty}^{1/4}/a = 0.753$. For the adiabatic walled infinite cylinder, there holds $N_{Ra1_\infty}^{1/4} = 16(67.9)\,(L/d)^4$, while $a = 7.66\,(L/d)$. Again, $N_{Ra1_\infty}^{1/4}/a \doteq 0.75$. However, it is not known whether the infinite roll is a physically realistic mode of convection, since a more unstable mode of convection is indicated by the Equation (14a) separation of variables approximation. For perfectly conducting walls, $N_{Ra1_\infty}^{1/4}/a = 1$ appears to be good. Predictions of the critical Rayleigh number for the infinite slot with adiabatic walls is compared with the work of Yih (*8*), Samuels and Churchill (*17*), and Kurzweg (*18*) in Table 5. The equivalent wave number approximation with $b_1 = \pi + 0.85$ yields results that are within 10% of the finite difference approximations presented by Samuels and Churchill. The results are also within 10% of those of Kurzweg for L/H of 1.0 and 2.0. Yih's results also compare well with $b_1 = \pi$, which is the appropriate value for free surface boundary conditions.

The theoretical predictions of the initiation Rayleigh number for the perfectly conducting wall case compare favorably with the experimental data of Catton and Edwards (*13*) for L/d greater than 1.0. For the case of adiabatic walls, the results compare favorably for L/d greater than 1.5, see Figure 1. As expected, the intermediate regime is affected by both the vertical and horizontal surfaces, and the method of separation of variables cannot be used.

The adjusted wave number method can be used in both cases to obtain predictions for the low L/d, and in both cases the predictions are never more than 10% low. At the high L/d, where the high L/d solutions are valid, the adjusted wave number method is equally good.

SUMMARY AND CONCLUSIONS

Tables 1, 3, and 4 give critical Rayleigh numbers for low L/d, square or circular cylinders and high L/d circular cylinders. These results are well represented by Equation (22) together with Equations (23) and (38), which give an equivalent wave number for right circular cylinders.

The adjusted wave number solution gives predictions that compare very well with the experimental results of Catton and Edwards (*13*) over the entire range of L/d considered.

ACKNOWLEDGMENT

Preliminary work on this paper was supported by National Science Foundation to which grateful acknowledgment is made.

This work is based in part on a Ph.D. thesis of Ivan Catton carried out in the Morrin-Martinelli-Gier Heat Transfer Laboratory of the University of California, Los Angeles. Grateful acknowledgment is made for support by the National Science Foundation in the initial stages of the work and for use of the UCLA Computing Center facilities.

NOTATION

a = horizontal wave number
A_m = constant of integration

A_n = constant of integration
b = vertical wave number
b_r = vertical wave number based on radius
B_1 = constant of integration, Equation (B-9)
B_2 = constant of integration, Equation (B10)
B_m = constant of integration
B_n = constant of integration
C = constant of integration
C_p = specific heat at constant pressure
D = $\partial/\partial z$
D_r = $\partial/\partial r$
D_r' = $\left(\frac{\partial}{\partial r} + \frac{1}{r}\right)$
f_m = function of x
f_{mn} = function of x and y
f_n = function of y
F = function of r, Equation (29)
F_s = function of A, Equation (A17)
g = gravitational acceleration
$g(z)$ = function of z
G_s = function of a and λ, Equation (A17)
H = side of a square or width of a slot
i = unit imaginary number
I_n = modified Bessel function of the first kind of order n
J_n = Bessel function of the first kind of order n
k = unit vector in z direction
k = z mode number
K = thermal conductivity
K_w = wall conductivity
L = cell height
L_r = cell height-to-radius ratio
m = horizontal mode number
n = unit vector normal to wall
n = horizontal mode number
N_{Ra} = Rayleigh number ($\alpha g\beta L^4/\kappa\nu$)
N_{Ra}^* = Rayleigh number based on cell radius ($\alpha g\beta d^4/16\kappa\nu$)
p = perturbation exponent
P = pressure
r = radial coordinate
t = time
t_w = wall thickness
T = temperature
T' = temperature disturbance
T_c = top cold temperature
T_h = bottom hot temperature
u = x velocity component
u' = disturbance in u
U = function of r, Equation (29)
v = velocity vector
v = y velocity component
v' = disturbance in v
V = function of r, Equation (29)
w = z velocity component
w' = disturbance in w
W = function of r, Equation (29)
x = horizontal coordinate
y = horizontal coordinate
z = vertical coordinate

Greek Letters

α = volume thermal expansion coefficient
β = temperature gradient in negative z direction
γ = parameter, Equation (A12)
δ = parameter, Equation (A12)
ϵ = parameter, Equation (A12)
ζ = parameter, Equation (A12)
η = parameter, Equation (A12)
θ = azimuthal angle from x axis
κ = thermal diffusivity
λ = parameter, Equation (A3)
Λ = function of r, Equation (29)
μ = viscosity
μ_j = characteristic root
ν = kinematic viscosity
π = 3.1415 . . .
ρ = fluid density
ψ = function of μ_j and b_r, Equation (B16)

LITERATURE CITED

1. Benard, H., *Rev. Gen. Sci. Pures Appl.*, **11**, 1261-71 (1900).
2. Rayleigh, Lord, *Phil. Mag.*, **32**, 529-46 (1916).
3. Pellew, A., and R. V. Southwell, *Proc. Roy. Soc. (London)*, **A176**, 312-43 (1940).
4. Malkus, W. V. R., *ibid.*, **A225**, 185-212 (1954).
5. ———, and G. Veronis, *J. Fluid Mech.*, **4**, 225-60 (1958).
6. Catton, Ivan, *Phys. Fluids*, **9**, 2521-22 (1966).
7. Ostrach, S., and D. Pneuli, *J. Heat Transfer*, **85**, 346-54 (1963).
8. Yih, Chia-Shun, *Quart. Appl. Math.*, **17**, No. 1, 25-42 (1959).
9. Ostroumov, G. A., *NACA Tech Memo 1407*, (Translation of "Svobodnaya Convectzia V Ousloviakh Vnoutrennei Zadachi," 1952), (1958).
10. Soberman, R. K., *J. Appl. Phys.*, **29**, 872-3 (1958).
11. Globe, S., and D. Dropkin, *Trans. Am. Soc. Mech. Engrs.*, **C81**, 24-8 (1959).
12. Slavnov, V. V., *Zh. Tekhn. Fiz.*, **26**, No. 9, 1938-1941 (1956).
13. Catton, Ivan, and D. K. Edwards, *J. Heat Transfer*, **87**, 295-299 (1967).
14. Chandrasekhar, S., "Hydrodynamic and Hydromagnetic Stability," pp. 9-73, Oxford at the Clarendon Press, England (1961).
15. Ostrach, S., "Theory of Laminar Flows," F. K. Moore, ed., Princeton Univ. Press, Princeton, N. J. (1964).
16. Sherman, M., and S. Ostrach, *J. Fluid Mech.*, **24**, 661-671 (1966).
17. Samuels, M. R., and S. W. Churchill, *AIChE J.*, **13**, No. 1, 77-85 (1967).
18. Kurzweg, U., *Intern. J. Heat Mass Transfer*, **1**, 35-41 (1965).

Manuscript received September 13, 1968; revision received December 20, 1968; paper accepted December 26, 1968.

APPENDIX A: SOLUTION OF THE LINEARIZED PERTURBATION EQUATIONS WITH APPROXIMATE SIDE WALL CONDITIONS

Pellew and Southwell Solution

When the approximate boundary conditions Equation (14*a*) are employed in place of Equation (14) to accommodate Equation (18), the characteristic equation to Equation (13) is indicated by Equation (20):

$$(4\mu_j^2 - a^2)^3 = -a^2 N_{Ra} \tag{A1}$$

where

$$w' = f(x,y)\, g(z)$$

$$g(z) = \sum_{j=1}^{3} C_j e^{\pm 2\mu_j z} \tag{A2}$$

For convenience, λ is defined by

$$a^2 N_{Ra} = \lambda^3 a^6 \text{ or } \lambda = (N_{Ra}/a^4)^{1/3} \tag{A3}$$

so that the roots of Equation (A1) may be written as

$$\begin{aligned} 4\mu_1^2 &= a^2(1 + \lambda e^{i3\pi/3}), \quad 2\mu_1 = ia(\lambda - 1)^{1/2} \\ 4\mu_2^2 &= a^2(1 + \lambda e^{i5\pi/3}), \quad 2\mu_2 = a(A - iB) \\ 4\mu_3^2 &= a^2(1 + \lambda e^{i\pi/3}), \quad 2\mu_3 = 2\mu_2^* \end{aligned} \tag{A4}$$

where $i = \sqrt{-1}$, the asterisk denotes the complex conjugate,

and A and B are given by

$$A^2 - B^2 = 1 + \lambda/2 \tag{A5}$$

$$2AB = \sqrt{3}\,\lambda/2 \tag{A6}$$

The terms in Equation (A2) can be combined in two ways to yield an even or an odd solution:

$$g(z) = C_1' \cosh(2\mu_1 z) + C_2' \cosh(2\mu_2 z) + C_3' \cosh(2\mu_2^* z)$$
$$g(z) = C_1'' \sinh(2\mu_1 z) + C_2'' \sinh(2\mu_2 z) + C_3'' \sinh(2\mu_2^* z) \tag{A7}$$

Either solution must meet the boundary conditions, which must be expressed in terms of w:

$$w'(z = \pm\tfrac{1}{2}) = 0$$
$$Dw'(z = \pm\tfrac{1}{2}) = 0$$
$$\nabla^4 w'(z = \pm\tfrac{1}{2}) = 0 \tag{A8}$$

The first equation follows from Equation (14); the second is derived from Equations (14) and (1); and the third follows from Equations (15) and (11). For the even solution, Equation (A8) requires

$$C_1' \cosh\mu_1 + C_2' \cosh\mu_2 + C_3' \cosh\mu_2^* = 0$$
$$\mu_1 C_1' \sinh\mu_1 + \mu_2 C_2' \sinh\mu_2 + \mu_2^* C_3' \sinh\mu_2^* = 0$$
$$(4\mu_1^2 - a^2)^2 C_1' \cosh\mu_1 + (4\mu_2^2 - a^2)^2 C_2' \cosh\mu_2 + (4\mu_2^{*2} - a^2)^2 C_3' \cosh\mu_2^* = 0 \tag{A9}$$

For this set of equations to have a nontrivial solution, the secular determinant must be zero:

$$\begin{vmatrix} \cosh\mu_1 & \cosh\mu_2 & \cosh\mu_2^* \\ \mu_1 \sinh\mu_1 & \mu_2 \sinh\mu_2 & \mu_2^* \sinh\mu_2^* \\ (4\mu_1^2 - a^2)^2 \cosh\mu_1 & (4\mu_2^2 - a^2)^2 \cosh\mu_2 & (4\mu_2^{*2} - a^2)^2 \cosh\mu_2^* \end{vmatrix} = 0 \tag{A10}$$

To simplify Equation (A10), the first row is converted to ones; each element in the first column is divided by $\cosh\mu_1$, those in the second by $\cosh\mu_2$, and the third by $\cosh\mu_2^*$. Equations (A4) for μ_1 and μ_2 are substituted into the third row, and each element in the row is divided by $a^4\lambda^2$. Then the third row has subtracted from each of its elements the elements (unity) in the first row. Dividing the third row by $-\sqrt{3/2}$ and expanding the determinant, we get

$$2ia(\lambda - 1)^{1/2} \tan[a(\lambda - 1)^{1/2}] + (\sqrt{3} + i)\mu_2 \tanh\mu_2 - (\sqrt{3} - i)\mu_2^* \tanh\mu_2^* = 0 \tag{A11}$$

For positive $(\lambda - 1)$, Equations (A11) contains only imaginary numbers, as the last two terms are the difference between a complex number and its complex conjugate.

Equation (A11) is put into a form so that its behavior is seen better by substituting Equations (A4) through (A6) and by arranging the terms into the following groups:

$$2\zeta/a = (\lambda - 1)^{1/2} = \left\{\frac{4A^2}{3}\left[2\left(1 - \frac{3}{4A^2}\right)^{1/2} - 1\right] - 1\right\}^{1/2}$$

$$\eta = A(\lambda - 1)^{-1/2} = A(2\zeta/a)^{-1}$$

$$\epsilon = B(\lambda - 1)^{-1/2} = \frac{\sqrt{3}}{4A}\left[\left(\frac{2\zeta}{a}\right)^2 + 1\right]\left(\frac{2\zeta}{a}\right)^{-1}$$

$$\gamma = \frac{A + \sqrt{3}B}{(\lambda - 1)^{1/2}} = 2A\left(\frac{2\zeta}{a}\right)^{-1}\left(1 - \frac{3}{4A^2}\right)^{1/2}$$

$$\delta = \frac{\sqrt{3}A - B}{(\lambda - 1)^{1/2}} = -\frac{4A}{\sqrt{3}}\left[2\left(1 - \frac{3}{4A^2}\right)^{1/2} - 1\right]\left(\frac{2\zeta}{a}\right)^{-1} \tag{A12}$$

The secular equation for the even solutions [Equation (A11)] can then be expressed as

$$-\tan\zeta = \frac{\gamma \sinh 2\eta\zeta + \delta \sin 2\epsilon\zeta}{\cosh 2\eta\zeta + \cos 2\epsilon\zeta} \tag{A13a}$$

In a similar way, the odd solution in Equation (A7) can be treated to yield

$$\cot\zeta = \frac{\gamma \sinh 2\eta\zeta - \delta \sin 2\epsilon\zeta}{\cosh 2\eta\zeta - \cos 2\epsilon\zeta} \tag{A13b}$$

These equations can be solved numerically by considering η, ϵ, γ, and δ as functions of ζ/a, through parameter A, and for a particular a by finding the intersections of the tangent and cotangent with the right side of Equations (A13a) and (A13b), respectively. In this way, Pellew and Southwell found the first six intersections for $a = 2, 3, 4$, and 5. A high-speed digital computer was used to extend the results of Pellew and Southwell for the first mode to wave numbers of 54. The results with eight significant figures of accuracy are presented in Table 1.

Approximate Closed Form Solution

For practical applications, we desire a simple approximate expression for the Rayleigh number as a function of a that is correct near the minimum Rayleigh number. For an exact result, we would utilize Equation (A4) for $N_{Ra}(a)$, the derivative of $N_{Ra}(a)$ set equal to zero, and Equations (A3) and (A12) giving A as a function of a:

$$N_{Ra} = a^4\lambda^3 \tag{A14}$$

$$\frac{dN_{Ra}}{da} = 0 \tag{A15}$$

$$\lambda = \frac{4A^2}{3}\left[2\left(1 - \frac{3}{4A^2}\right)^{1/2} - 1\right] \tag{A16}$$

$$G_s(a,\lambda) = -\tan\frac{a\sqrt{\lambda - 1}}{2} = F_s(A) = \frac{\gamma \sinh 2\eta\zeta + \delta \sin 2\epsilon\zeta}{\cos 2\eta\zeta + \cos 2\epsilon\zeta} \tag{A17}$$

Instead, the approximation is introduced that $F_s(A)$ is a slowly varying function of A, so that its derivative may be neglected compared with $-dG_s/da$. The value of $F_s(A)$ taken is the one at the first intersection, $F_s = 2.22$. Equations (A17) and (A14) then yield

$$\frac{1}{2}a\sqrt{\lambda - 1} = \frac{k\pi}{2} + 0.423$$

$$N_{Ra} = a^4\lambda^3 = \frac{[(k\pi + 0.85)^2 + a^2]^3}{a^2} \tag{A18}$$

where k is an odd integer for an even velocity profile. Equation (A18) holds for both the odd and even solutions, since Equation (A13b) with right side taken equal to 2.22 yields the same result with k an even integer.

APPENDIX B: SOLUTION OF THE LINEARIZED PERTURBATION EQUATIONS WITH APPROXIMATE END CONDITIONS

Equations (31) to (35), subject to boundary conditions via Equation (29), or Equations (14b) and either (16) or (17) constitute the set for which solutions are sought. Equation (33) is a sixth-order linear ordinary differential equation in W alone. The other equations in the set are needed only for applications of the boundary conditions. Some of the original conservation equations, Equations (1) through (3), will be needed to interrelate the constants of integration.

The solution to Equations (33) having no singularities at $r = 0$ is

$$W = \sum_{j=1}^{3} C_j J_n(\mu_j r) \tag{B1}$$

where μ_j^2 are roots of the characteristic equation

$$(\mu_j^2 + b_r^2)^3 - \mu_j^2 N_{Ra}^* = 0 \qquad \text{(B2)}$$

and J_n is the Bessel function of the first kind of order n. For convenience, the parameter λ is introduced to simplify Equation (B2):

$$\lambda = \mu_j^2 + b_r^2 \qquad \text{(B3)}$$

There results

$$\lambda^3 - N_{Ra}^*\lambda + b_r^2 N_{Ra}^* = 0 \qquad \text{(B4)}$$

For the expected condition $N_{Ra}^* \geq (27/4)b_r^4$, the roots to Equation (B4) are

$$\lambda_1 = \frac{2}{\sqrt{3}}\sqrt{N_{Ra}^*}\cos(\gamma/3)$$

$$\lambda_2 = \frac{2}{\sqrt{3}}\sqrt{N_{Ra}^*}\cos[(\gamma + 2\pi)/3]$$

$$\lambda_3 = -\frac{2}{\sqrt{3}}\sqrt{N_{Ra}^*}\cos[(\gamma + \pi)/3] \qquad \text{(B5)}$$

where

$$\cos\gamma = -\frac{3^{3/2}b_r^2}{2\sqrt{N_{Ra}^*}} \qquad \text{(B6)}$$

Equation (32) then indicates that the particular solution for F, which satisfies the original energy equation, is

$$F = \sum_{j=1}^{3} C_j \frac{(\mu_j^2 + b_r^2)^2}{\mu_j^2 N_{Ra}^*} J_n(\mu_j r) \qquad \text{(B7)}$$

Equation (31) and the original z momentum equation likewise indicate

$$\Lambda = \sum_{j=1}^{3} C_j \frac{(\mu_j^2 + b_r^2)b_r}{\mu_j^2} J_n(\mu_j r) \qquad \text{(B8)}$$

In addition to the particular solution to Equation (34), the nonsingular term from the general solution must be admitted:

$$U + V = B_1 I_{n+1}(b_r r) + b_r \sum_{j=1}^{3} (C_j/\mu_j) J_{n+1}(\mu_j r) \qquad \text{(B9)}$$

Similarly, Equation (35) indicates

$$U - V = B_2 I_{n-1}(b_r r) - b_r \sum_{j=1}^{3} (C_j/\mu_j) J_{n-1}(\mu_j r) \qquad \text{(B10)}$$

where B_2 must be related to B_1 by one of the original conservation equations not already used to interrelate constants of integration. Continuity, Equation (4), is well suited for this purpose. Substitution of Equations (B9), (B10), and (B1) into Equation (1) yields

$$B_1 = -B_2 \qquad \text{(B11)}$$

Application of the boundary conditions $U = V = 0$ at $r = 1$ permits B_1 and B_2 to be eliminated entirely.

$$B_1 = \frac{-b_r}{I_{n+1}(b_r)} \sum_{j=1}^{3} \frac{C_j}{\mu_j} J_{n+1}(\mu_j) = -B_2$$

$$= \frac{-b_r}{I_{n-1}(b_r)} \sum_{j=1}^{3} \frac{C_j}{\mu_j} J_{n-1}(\mu_j)$$

$$\sum_{j=1}^{3} (C_j/\mu_j) \left[\frac{J_{n+1}(\mu_j)}{I_{n+1}(b_r)} - \frac{J_{n-1}(\mu_j)}{I_{n-1}(b_r)} \right] = 0 \qquad \text{(B12)}$$

The other boundary conditions are

$$W(1) = 0, \quad \sum_{j=1}^{3} C_j J_n(\mu_j) = 0 \qquad \text{(B13)}$$

Adiabatic wall, $D_r F(1) = 0$:

$$\sum_{j=1}^{3} C_j \frac{(\mu_j^2 + b_r^2)^2 J_n'(\mu_j)}{\mu_j} = 0 \qquad \text{(B14}a\text{)}$$

For a perfectly conducting wall, $F(1) = 0$:

$$\sum_{j=1}^{3} C_j \frac{(\mu_j^2 + b_r^2)^2}{\mu_j^2} J_n(\mu_j) = 0 \qquad \text{(B14}b\text{)}$$

where $J_n'(\mu_j)$ is $dJ_n(x)/dx$ evaluated at $x = \mu_j$.

For a nontrivial solution to Equation (B12) through (B14), the secular determinant must be zero. The secular equation for the adiabatic wall is

$$\begin{vmatrix} \underset{\psi_1}{\dfrac{J_n(\mu_1)}{\dfrac{(\mu_1^2 + b_r^2)^2}{\mu_1} J_n'(\mu_1)}} & \underset{\psi_2}{\dfrac{J_n(\mu_2)}{\dfrac{(\mu_2^2 + b_r^2)^2}{\mu_2} J_n'(\mu_2)}} & \underset{\psi_3}{\dfrac{J_n(\mu_3)}{\dfrac{(\mu_3^2 + b_r^2)^2}{\mu_3} J_n'(\mu_3)}} \end{vmatrix} = 0 \qquad \text{(B15)}$$

where ψ_1 is a term multiplied by C_j in Equation (B12):

$$\psi_j = \frac{1}{\mu_j}\left[\frac{J_{n+1}(\mu_j)}{I_{n+1}(b_r)} - \frac{J_{n-1}(\mu_j)}{I_{n-1}(b_r)} \right] \qquad \text{(B16)}$$

When $b_r = 0$, that is, $L/d = \infty$, the secular equation becomes that presented by Yih (*8*):

$$\mu_2^3 J_n(\mu_1) J_n'(\mu_2) - \mu_1^3 J_n'(\mu_1) J_n(\mu_2) = 0 \qquad \text{(B17)}$$

where $\mu_1 = N_{Ra}^{*1/4}$ and $\mu_2 = N_{Ra}^{*1/4}$ from Equations (B3) and (B4).

For the perfectly conducting wall, the secular equation is

$$\begin{vmatrix} \underset{\psi_1}{\dfrac{J_n(\mu_1)}{\dfrac{(\mu_1^2 + b_r^2)^2}{\mu_1^2} J_n(\mu_1)}} & \underset{\psi_2}{\dfrac{J_n(\mu_2^2)}{\dfrac{(\mu_2^2 + b_r^2)^2}{\mu_2^2} J_n(\mu_2)}} & \underset{\psi_3}{\dfrac{J_n(\mu_3)}{\dfrac{(\mu_3^2 + b_r^2)^2}{\mu_3^2} J_n(\mu_3)}} \end{vmatrix} = 0 \qquad \text{(B18)}$$

If $b_r = 0$, the equation becomes that presented by Ostrach (*15*):

$$J_n(\mu_1) = 0 \qquad \text{(B19)}$$

For a particular b_r and n, the value of N_{Ra}^* was found from Equations (B15) or (B19) numerically with the aid of a high-speed computer. The determinant was computed as N_{Ra}^* and was increased in large steps until a change of sign was found. Then N_{Ra}^* was reduced in smaller steps until the sign changed back, and this process was repeated until eight significant figures in N_{Ra}^* were obtained. The lowest values of N_{Ra}^* were found when $n = 1$ and $k = 1$.